

THERMAL PERFORMANCE ANALYSIS OF CIRCULAR ABSORBER TUBE OF PARABOLIC TROUGH COLLECTOR USING PERFORATED VORTEX GENERATING INSERTS

Utkarsh Mishra^a, Sanjeev Kumar Joshi^b

^a Research Scholar, Department of Mechanical Engineering, Uttarakhand University, Dehradun, Uttarakhand

^b Assistant Professor, Department of Mechanical Engineering, Uttarakhand University, Dehradun, Uttarakhand

ABSTRACT

The Numerical Investigation is carried out on the Circular Absorber Tube of Parabolic Trough Collector using Perforated Vortex Generator Inserts. These inserts are of the shape of the Cut Cone (Delta Wing Shaped) types mounted on the opposite side of the central rod at the specific axial location with the help of the pinned rod. The Inserts used, induces the vortex in the flow which disrupts the growth of Thermal boundary. Air is used as the working fluid and heat transfer measurements for both smooth and rough surface sides of the tube are reported for fully developed turbulent flow with Reynolds number (Re) varying between 10,000 and 50,000. The variation of the Nusselt Number (Nu) with respect to Reynolds Numbers (Re) is investigated at various ratios of Relative Roughness Height (e/D_h) and P_c/C_L . Effect of Vortex Generation on the Friction Factor has also been investigated in the Analysis for different ratios of Relative Roughness Height (e/D_h) at the specified pitch lengths of 60 mm and 45 mm respectively.

1. Introduction

Numerical Analysis has been performed to investigate for the enhancement of heat in the Absorber Tube of the Parabolic Trough Collector using inserts of the shape of the Cut Cones or Delta Wings. The experiment proceeds with certain modifications in the set up which includes incorporation of the additional perforations ranging from no perforation to Double and than Triple in the inserts i.e. $n = 0, 2$ & 3 , the pitch P_c between the inserts has also been used as 45 mm and 60 mm at variable Relative Roughness Height (e/D_h). The results of the investigation have been realized on the Nusselt Number (Nu) and the Friction Factor (F_f) at Reynolds Numbers (Re) varying from 10,000-50,000. The over scheme of the experiment is aimed to increase the vortex in the fluid passing in the absorber tube which delimits the formation of the Thermal Boundary layer which eventually would increase the rate of convective heat transfer and would ultimately increase the overall thermal efficacy of the system.

2. Geometric Details of the Set up

A Copper absorber Tube of length (L) 1000 mm, Internal Diameter (D_i) 25 mm and Outer Diameter (D_o) 30 mm has been taken in which the copper inserts of the shape of cut cones or delta wings have been inserted whose thickness are 0.5 mm. The inserts are mounted on the pinned rod which is eventually connected to the central rod through welding. The Diameter of the Central Rod is 2 mm and the same of the Pinned Rod is 1 mm.

For the investigation purpose, following modification has been incorporated in the set up:

- i. A variable pitch of 45 mm and 60 mm has been taken at which readings has been taken individually.

- ii. The number of Perforations on the inserts have been taken from no perforation to Double and than Triple i.e. $n=0, 2$ and 3 .
- iii. The Variation in Roughness Height (e) of the cutting cones has been taken ranging from 4 mm, 6 mm and 8 mm so that the Relative Roughness to Hydraulic Ratio e/D_h is 0.27, 0.20 and 0.133.

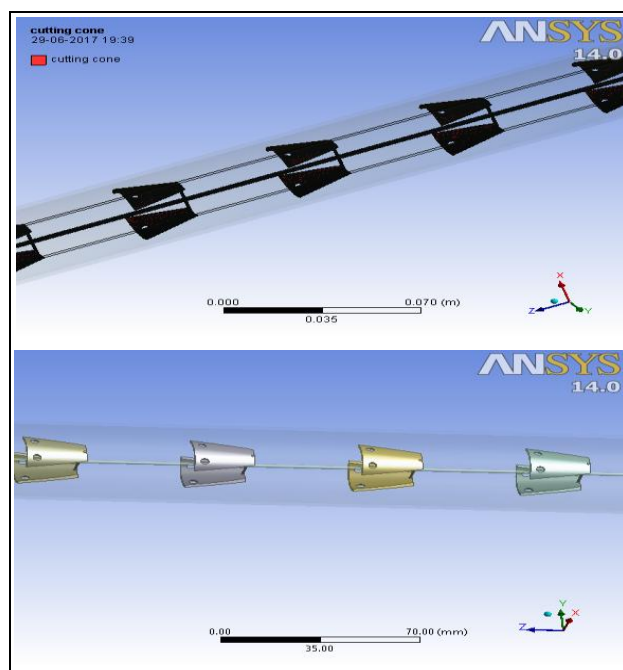


Fig.2.1 Complete Geometric Model of the Absorber Tube with Cutting Cones as the Inserts

3. Numerical Analysis Methodologies

The numerical and thermal performance analysis and simulation of the Circular Absorber tube of Parabolic Trough Collector using perforated vortex generator insert is done on the basis of computational fluid dynamics (CFD). The aim of the CFD or run of the CFD code – Ansys fluent to generate the design and generate the good meshing if the boundary condition and model parameters do not in properly applied, So Ansys Fluent 14.0 CFD algorithms used. The Absorber Tube with the Perforated Inserts is designed in ANSYS FLUENT 14.0 with Realizable k-ε Model, an improved version over the Standard k-ε Model. This model is also capable of precisely computing turbulent flows which was necessary for handling our Analysis where the Range of the Reynolds Number is taken to be from 10,000-50,000.

4. Assumptions & Mathematical Foundation

The numerical model for fluid flow and heat transfer in a channel was developed under the following assumptions:

- i. Steady flows
- ii. Pressure variation in y direction is zero.
- iii. Shear force in y direction is zero.
- iv. Body force due to gravity has been neglected.
- v. Incompressible flow.
- vi. At the inlet of test section, the flow has been fully developed flow
- vii. The axial heat conduction in the fluid was negligible.
- viii. The properties of air were constant at atmospheric pressure and temperature

Based on the above assumptions, the channel flow is governed by the Continuity Equation, The Navier Stokes Equations and The Energy Equation.

Continuity Equation:

$$\frac{\partial \bar{u}}{\partial x} + \frac{\partial \bar{v}}{\partial y} + \frac{\partial \bar{w}}{\partial z} = 0$$

Momentum Equation:

X- Momentum Equations:

$$\left(\bar{u} \frac{\partial \bar{u}}{\partial x} + \bar{v} \frac{\partial \bar{u}}{\partial y} + \bar{w} \frac{\partial \bar{u}}{\partial z}\right) = -\frac{1}{\rho} \frac{\partial p}{\partial x} + \nu \left(\frac{\partial^2 \bar{u}}{\partial x^2} + \frac{\partial^2 \bar{u}}{\partial y^2} + \frac{\partial^2 \bar{u}}{\partial z^2}\right)$$

Y- Momentum Equation:

$$\left(\bar{u} \frac{\partial \bar{v}}{\partial x} + \bar{v} \frac{\partial \bar{v}}{\partial y} + \bar{w} \frac{\partial \bar{v}}{\partial z}\right) = -\frac{1}{\rho} \frac{\partial p}{\partial y} + \nu \left(\frac{\partial^2 \bar{v}}{\partial x^2} + \frac{\partial^2 \bar{v}}{\partial y^2} + \frac{\partial^2 \bar{v}}{\partial z^2}\right)$$

Z – Momentum Equations:

$$\left(\bar{u} \frac{\partial \bar{w}}{\partial x} + \bar{v} \frac{\partial \bar{w}}{\partial y} + \bar{w} \frac{\partial \bar{w}}{\partial z}\right) = -\frac{1}{\rho} \frac{\partial p}{\partial z} + \nu \left(\frac{\partial^2 \bar{w}}{\partial x^2} + \frac{\partial^2 \bar{w}}{\partial y^2} + \frac{\partial^2 \bar{w}}{\partial z^2}\right)$$

Energy Equation:

$$\bar{u} \frac{\partial t}{\partial x} + \bar{v} \frac{\partial t}{\partial y} + \bar{w} \frac{\partial t}{\partial z} = \alpha \left(\frac{\partial^2 t}{\partial x^2} + \frac{\partial^2 t}{\partial y^2} + \frac{\partial^2 t}{\partial z^2}\right)$$

5. Result and Discussion

5.1. Validation of Numerical Data with Experimental Data

Following curve has been achieved showing congruency with the Experimental data. This shows the validation of the Numerical Analysis with the Experimental Data.

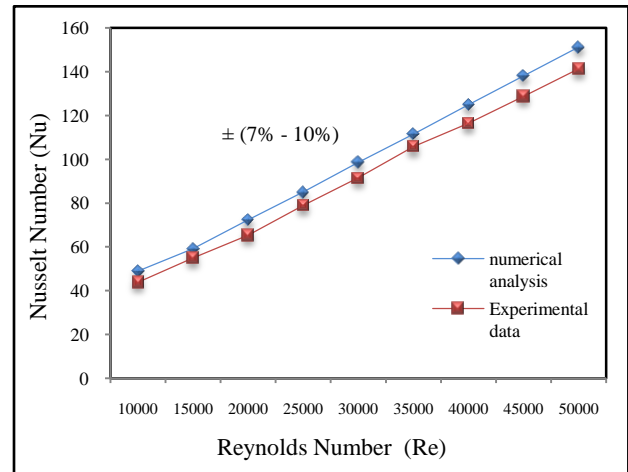


Fig 5.1.1 Validation of the Numerical Data with Experimental Data

5.2. Comparison Between Smooth Tube and Dittus-Boelter

The expression of Dittus-Boelter equation for the range of Reynolds Numbers taken in between 10000 to 50000 is given by $Nu_x = 0.023 \times Re^{0.8} \times Pr^{0.4}$

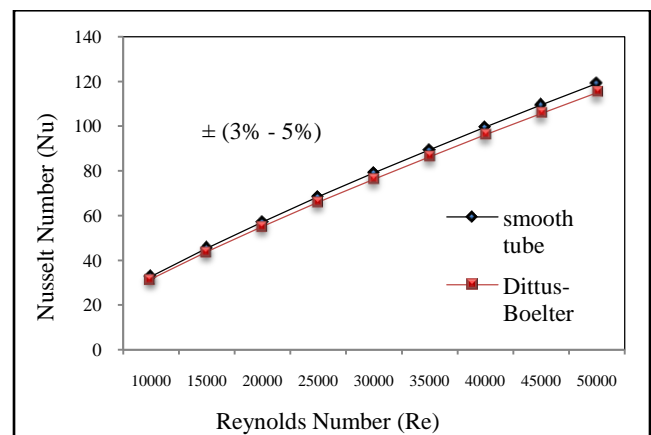


Fig 5.2.1 Comparison between Smooth Tube and Dittus-Boelter

5.3. Effect of Perforations and the Pitch

The effect on Nusselt Number with respect to Reynolds Number on addition the perforation on the Inserts

is counter on the rate of the Heat Transfer as we see from the trends that with decreasing number of holes i.e. from $n=3$ to $n=0$ there is an upward shift in the Nusselt Number. The upward shift is also supplemented with greater Roughness Ratio i.e. when the height of the conical skirt from the axis was taken as 8 mm ($e/D_h=8/30=0.27$) and greater pitch which is expressed as a function of $P_c/C_L=60/22=2.27$). The maximum value of Nusselt Number at $N=0$, $e/D_h=0.27$ and $P_c/C_L=2.27$ is 191.59. This is visible in the Fig. 5.3.1. The value of Nusselt Number for $N=3$ is least as 156.28 and the value for smooth tube is 119.05.

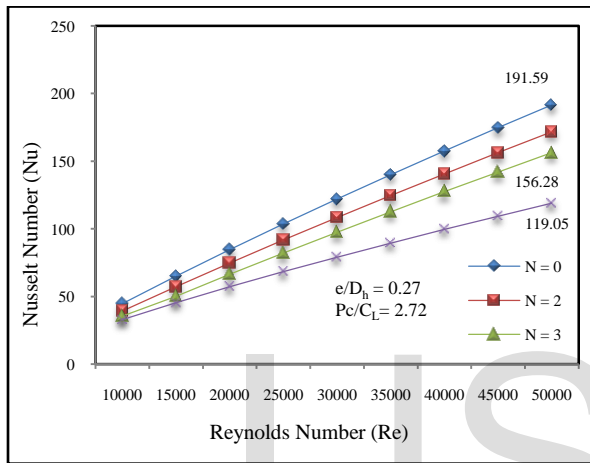


Fig. 5.3.1 Variation of Nusselt Number vs. Reynolds number (Re) at $P_c/C_L = 2.72$ and $e/D_h = 0.27$

The trend of the Nusselt Number with respect to the Reynolds Number could also be seen in the Fig. 5.3.2 i.e. when the height of the Cone Skirt to the axis is 6 mm i.e. $e/D_h=6/30=0.20$ and Pitch=60 mm which is manifested in the ratio form as $P_c/C_L=60/22=2.27$.

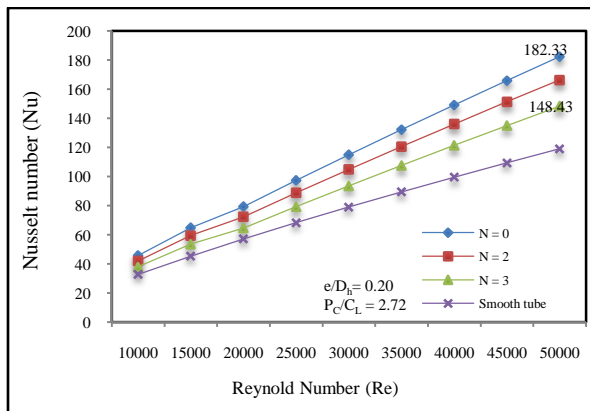


Fig. 5.3.2 Variation of Nusselt Number vs. Reynolds Number at $P_c/C_L = 2.72$ and $e/D_h = 0.20$

Fig 5.3.3 Show the variation of Nusselt Number with respect to Reynolds Number when the height of the Cone Skirt to the axis is 4 mm i.e. $e/D_h=4/30=0.133$ and Pitch=60 mm which is manifested in the ratio form as $P_c/C_L=60/22=2.27$.

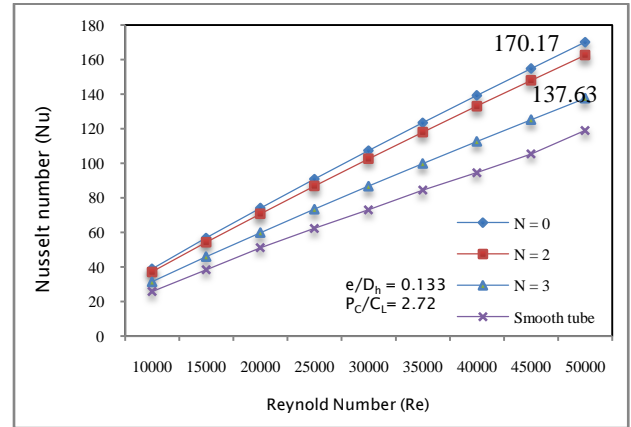


Fig. 5.3.3 Variation of Nusselt Number vs. Reynolds number (Re) at $P_c/C_L = 2.72$ and $e/D_h = 0.133$

The trends at Pitch $P_c=45$ mm expressed as the function of $P_c/C_L=45/22=2.04$ and height of the Cone Skirt to its Axis $e=8$ mm, 6mm and 4 mm which is expressed as a function of $e/D_h=0.27$, 0.20 and 0.133 respectively is shown in Fig 5.3.4, Fig 5.3.5 and Fig 5.3.5.

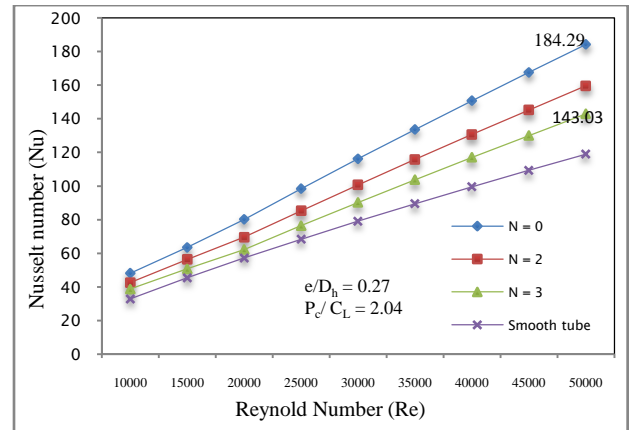


Fig. 5.3.4 Variation of Nusselt Number vs. Reynolds number (Re) at $P_c/C_L = 2.04$ and $e/D_h = 0.27$

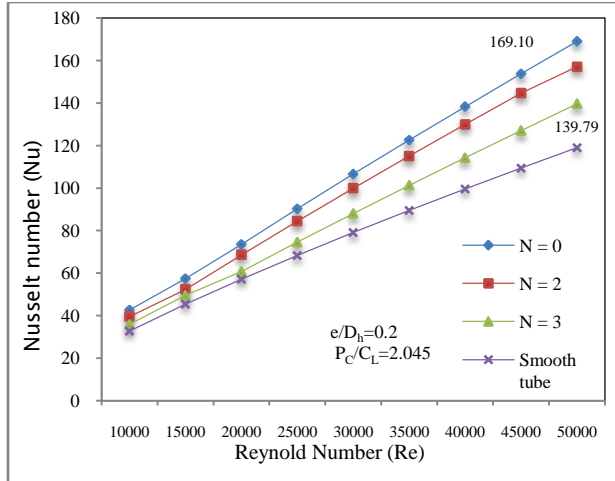


Fig. 5.3.4 Variation of Nusselt Number vs. Reynolds number (Re) at $P_C/C_L = 2.04$ and $e/D_h = 0.20$

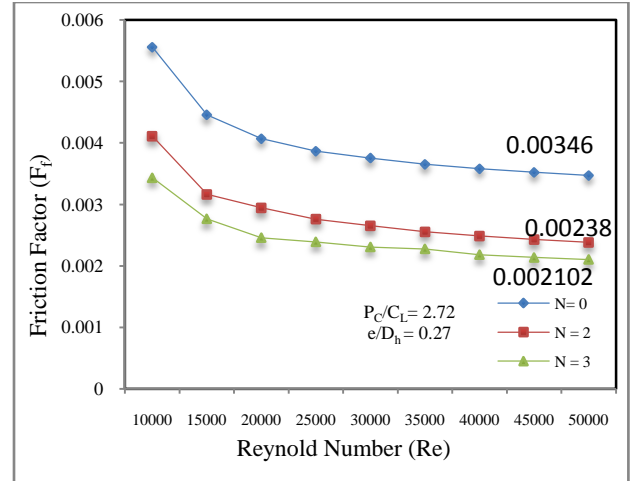


Fig 5.4.1 Variation of Friction Factor vs. Reynolds Number at $P_C/C_L=2.72$ and $e/D_h=0.27$

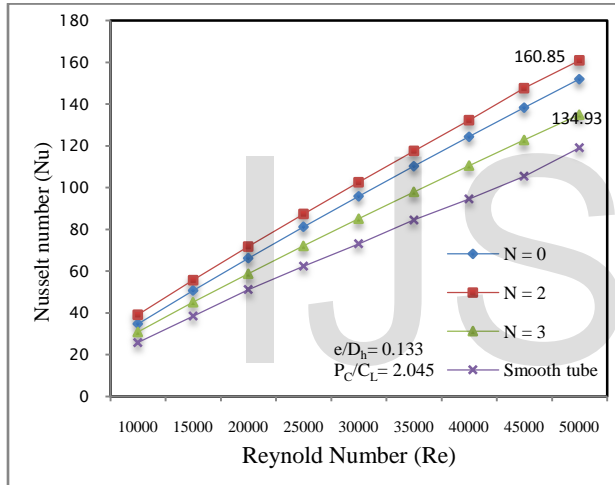


Fig. 5.3.5 Variation of Nusselt Number vs. Reynolds number (Re) at $P_C/C_L = 2.04$ and $e/D_h = 0.133$

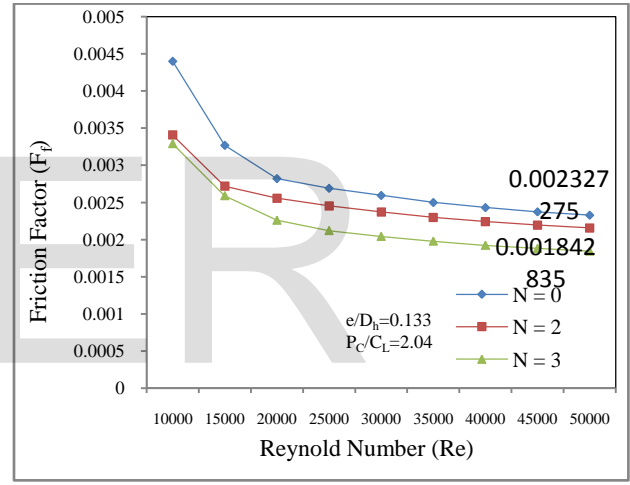


Fig 5.4.2 Variation of Friction Factor vs. Reynolds Number at $P_C/C_L=2.04$ and $e/D_h=0.133$

5.4 Effect of Perforation and Pitch on Friction Factor

The Friction factor (F_f) plays important roles in determining the efficacy of the design of the apparatus. Although the Friction Factor (F_f) mainly depends upon Reynolds Number and the Relative Roughness Ratio (e/D_h) per se, the role of perforations is not very significant in the determination of the Friction Factor (According to the Moody’s Diagram). The lesser values of Friction Factor (F_f) are favorable for the apparatus’ life.

Following are the results obtained from the three spatial permutations of the Inserts on the Nusselt Number as well as Friction factor (F_f) which in turns shows the enhancement in absorptivity of the flux.

The Friction Factor (F_f) decreases with the increase of the Reynolds Number as it is clear from the above trends. The trends also show that the value of Friction Factor (F_f) reduces as number of Perforations increases. In addition to this the lower values of the Friction Factor (F_f) are achieved at lower P_C/C_L ratio and e/D_h . The minimum value of Friction Factor (F_f) is achieved is 0.001842 at $N=3$, $P_C/C_L=2.04$ and $e/D_h=0.27$

6. Conclusion

The main conclusions of the above Numerical Investigation are as follows:

- i. The effect of Nusselt Number with respect to Reynolds Number on addition of perforations is contrary to the Heat Transfer is proportional i.e. The maximum value of

- Nusselt Number was obtained with no perforation ($N=0$). The value was 191.59.
- ii. The effect on Nusselt Number with respect to the Reynolds Number on increasing the Pitch P_c (which is manifested on as a function of P_c/C_L) is proportional. The maximum value of Nusselt Number obtained was 191.59 at $P_c/C_L=60/22=2.72$. In addition to this, the value was greatest with highest Roughness ratio which was manifested as functions of $e/D_h=8/30=0.27$.
 - iii. The value of Friction Factor (F_f) decreases with the increase in the Reynolds Number. It also reduces with addition of Perforations. The value of Friction Factor (F_f) reduces with lower values of Pitch and Roughness Height which are manifested in P_c/C_L and e/D_h . The minimum value of Friction Factor (F_f) is 0.001842 at $Re=50000$, $N=3$, $P_c/C_L=45/22=2.04$ and $e/D_h=4/30=0.133$.
 - iv. From the results, it is clear that realizable $k-\epsilon$ could provide results with acceptable engineering accuracy for the analysis of flow and heat transfer.

7. Nomenclature

Symbol	Meaning and Unit
L	Length of the Circular Tube (mm)
D_o	Outer Diameter of Circular Tube (mm)
D_i	Inner Diameter of Circular Tube (mm)
D_h	Equivalent Hydraulic Diameter of Tube (mm)
T	Air Temperature (K)
V	Air Velocity (m/s)
P	Density of Air (kg/m^3)
Pr	Prandtl Number
Re	Reynolds Number
Nu	Nusselt Number
q/A	Uniform Heat Flux (W/m^2)
e/D_h	Relative Roughness Height
ΔP	Pressure Difference (Pa)
C_p	Specific Heat ($J/kg.k$)
M	Mass Flow Rate of Air (Kg/s)
P_c	Pitch
C_L	Length of Cone, 2 mm
F_f	Friction Factor
C_{pCu}	Specific Heat of Copper ($J/kg.k$)
T	Time (s)
Q	Heat Transfer Rate (Kg/s)
U_i	Velocity at Inlet (m/s)
V_i	Velocity at Outlet (m/s)
e/H	Blockage Ratio

8. References

[1] C.Chang, C.Xu, Z.Y.Wu, X.Li, Q.Q.Zhang, Z.F.Wang, Heat transfer enhancement and performance of solar

thermal absorber tubes with circumferentially non-uniform heat flux, Energy Procedia 69 (2015) 320 – 327

[2] E. Bellos, C. Tzivanidis, K.A. Antonopoulos, G. Gkinis, Thermal enhancement of solar parabolic trough collectors by using nanofluids and converging-diverging absorber tube, Renewable Energy 94 (2016) 213-222.

[3] W. Fuqiang, T. Zhexiang, G. Xiangtao, T. Jianyu, H. Huaizhi, L. Bingxi, Heat transfer performance enhancement and thermal strain restrain of tube receiver for parabolic trough solar collector by using asymmetric outward convex corrugated tube, Energy 114 (2016) 275-292

[4] Sh. Ghadirijafarbigloo, A. H. Zamzaman, M. Yaghoubi, 3-D numerical simulation of heat transfer and turbulent flow in a receiver tube of solar parabolic trough concentrator with louvered twisted-tape inserts, Energy Procedia 49 (2014) 373 – 380

[5] K. Ravi Kumar, K.S. Reddy, Thermal analysis of solar parabolic trough with porous disc receiver, Applied Energy 86 (2009) 1804–1812

[6] K.S. Reddy, K. Ravi Kumar, C.S. Ajay, Experimental investigation of porous disc enhanced receiver for solar parabolic trough collector, Renewable Energy 77 (2015) 308-319

[7] G. Xiangtao, W. Fuqiang, W. Haiyan, T. Jianyu, L. Qingzhi, H. Huaizhi, Heat transfer enhancement analysis of tube receiver for parabolic trough solar collector with pin fin arrays inserting, Solar Energy 144 (2017) 185–202

[8] Z. Huang, G.L. Yu, Z.Y. Li, W.Q. Tao, Numerical study on heat transfer enhancement in a receiver tube of parabolic trough solar collector with dimples, protrusions and helical fins, Energy Procedia 69 (2015) 1306 – 1316

[9] M. T. Jamal-Abad, S. Saedodin, M. Aminy, Experimental investigation on a solar parabolic trough collector for absorber tube filled with porous media, Renewable Energy S0960-1481(2017)30081-2

[10] D. R.Waghole, R.M.Warkhedkar, V.S. kulkarni, R.K. Shrivastva, Experimental Investigations on Heat Transfer and Friction Factor of Silver Nanofluid in Absorber/Receiver of Parabolic Trough Collector with Twisted Tape Inserts, Energy Procedia 45 (2014) 558 – 567

[11] P.W. Deshmukh, S.V. Prabhu, R.P. Vedula, Heat transfer enhancement for laminar flow in tubes using curved delta wing vortex generator inserts, Applied Thermal Engineering 106 (2016) 1415–1426